Laboratory Work No. 15.
Spontaneous Fission of ^{252}Cf.

The aim of the work is to study the energy spectrum of the fragments from the spontaneous fission of ^{252}Cf *and to determine the ratio of decay probabilities for* ^{252}Cf *through different channels.*

Contents

1. Fission of atomic nuclei

The atomic nucleus is a system of protons and neutrons bound together by the *strong nuclear interaction*. By analogy with atoms and molecules, and in accordance with Einstein's famous formula $E = mc^2$, the mass of an atomic nucleus is determined not only by the mass of its constituent particles but also by the *binding energy*. However, compared to the binding energy in

atoms and molecules, the binding energy of atomic nuclei is many orders of magnitude higher. For example, in an atom, this energy is on the order of a few eV, whereas in a nucleus, typical binding energies are on the order of several MeV. Thus, chemical reactions (involving the breaking of molecular and atomic bonds) release roughly a million times less energy than nuclear reactions. Figure 1 shows the binding energies of different nuclei as a function of their mass.

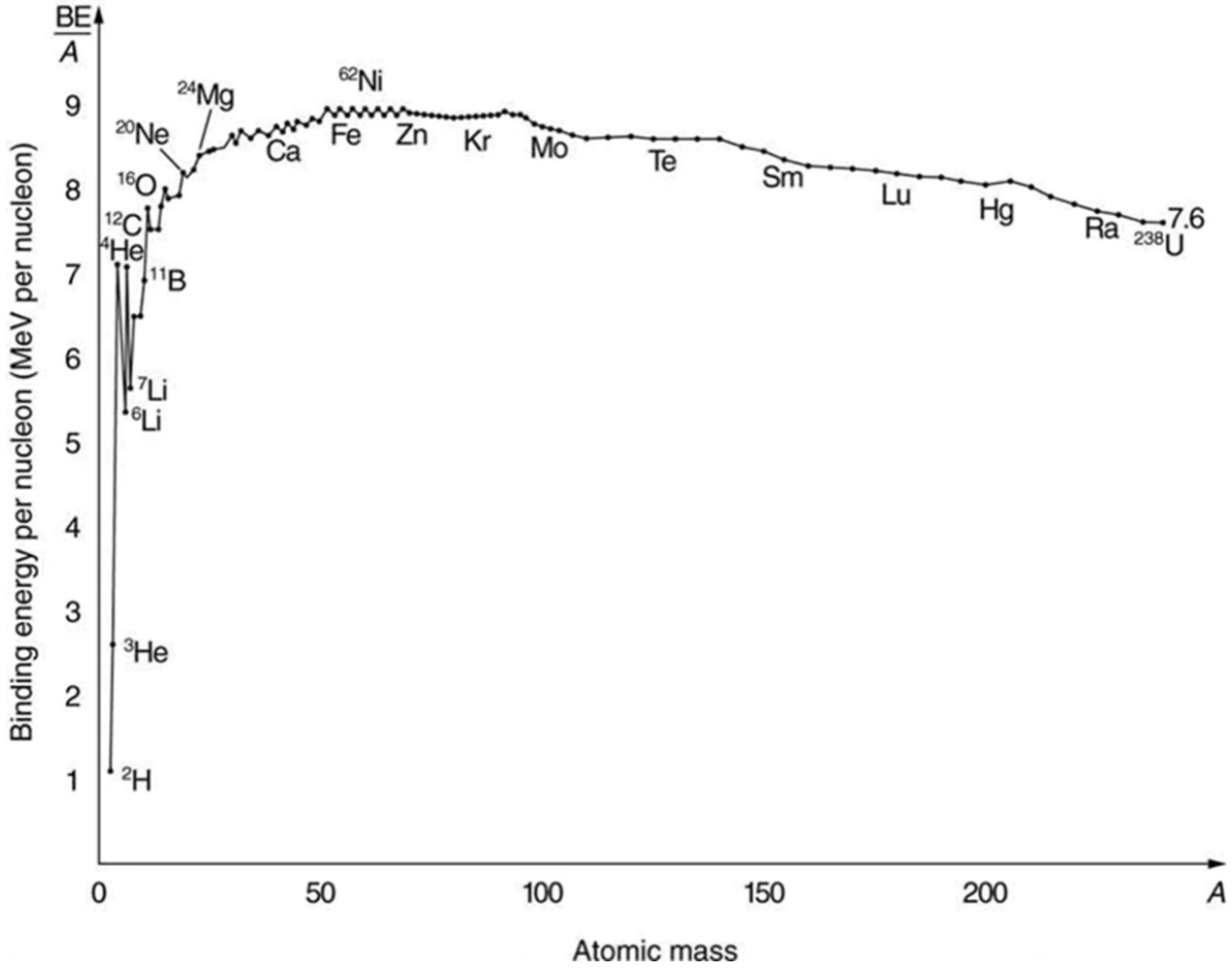

Figure 1. Binding energy of nuclei as a function of mass number.

As seen from this figure, the nuclear binding energy initially increases, reaches a maximum, and then gradually decreases. Thus, it can be said that the most stable nuclei are located near the maximum on this graph. This implies that, in principle, lighter nuclei may gain energy by merging (i.e., nuclear fusion occurs), while heavier nuclei may gain energy by splitting (i.e.,

nuclear fission occurs).

Fission can be spontaneous (similar to radioactive decay) or induced (e.g., as a result of neutron irradiation). For example, in this work, the ^{252}Cf (californium-252) nucleus undergoes spontaneous fission, whereas the well-known isotope ^{235}U (uranium-235), used in both nuclear power plants and nuclear weapons, does not fission on its own. It must be irradiated with slow neutrons (i.e., neutrons with thermal energies). This is why neutron moderators (such as graphite or heavy water) are crucial components in nuclear reactors.

2. Historical overview

In 1934, E. Fermi began experiments on irradiating uranium with slow neutrons from a radium-beryllium source. The goal of these experiments, which spurred numerous similar studies in other laboratories, was to discover transuranium elements – unknown at the time – that were expected to form as a result of β decay from uranium isotopes produced by neutron capture. New radioactive products were indeed found, but further research revealed that the radiochemical properties of many "new transuranium elements" differed from expectations.

Research into these unusual products continued until 1939, when radiochemists O. Hahn and F. Strassmann proved that the "new activities" belonged not to heavy elements, as initially thought, but to elements of intermediate atomic weight. The correct interpretation of this unusual nuclear process was provided the same year by L. Meitner and O. Frisch, who demonstrated that the excited uranium nucleus splits into two fragments. Based on an analysis of nuclear binding energies across the periodic table, they concluded that each fission event must release a large amount of energy (approximately 200 MeV) – several dozen times greater than that released in β decay.

This conclusion was confirmed by Frisch's experiments, which detected large signal pulses from fission fragments in an ionization chamber, and by

F. Joliot's measurements of fragment ranges, showing that they carried substantial kinetic energy.

In 1939, N. Bohr and J.A. Wheeler, as well as Soviet physicist Ya.I. Frenkel – long before fission was thoroughly studied experimentally – proposed a theoretical description of the process based on the liquid-drop model of the nucleus. This model provided a simple yet effective explanation for the fundamental features of fission. The basic principles of this model are outlined below.

The process of spontaneous fission in heavy nuclei was first discovered in uranium by G.N. Flerov and K.A. Petrzhak in 1940. Spontaneous fission is one of the types of radioactivity exhibited by atomic nuclei.

3. Elementary theory of fission

The atomic nucleus is an extremely complex quantum system. As previously mentioned, its particles are bound by the strong nuclear force. The strong interaction is difficult to describe theoretically because, unlike the electromagnetic force, its exact potential is not known. For this reason, nuclear models are used to describe the nucleus.

One of the earliest and simplest models is the liquid-drop model, proposed by N. Bohr in 1936, which treats the nucleus as a drop of charged fluid. Based on this model, C.F. von Weizsäcker derived a formula for nuclear binding energy (the semi-empirical mass formula):

$$W(A,Z) = a_1 A - a_2 A^{2/3} - a_3 \frac{Z^2}{A^{1/3}} - a_4 \frac{(A-2Z)^2}{A} + a_5 A^{-3/4}, \qquad (1)$$

where the coefficients are (in MeV): $a_1 = 15.8$, $a_2 = 17.8$, $a_3 = 0.72$, $a_4 = 23.7$, $a_5 = 34$ and

$$\delta = \begin{cases} 1 & \text{for even-even nuclei,} \\ 0 & \text{for odd-A nuclei,} \\ -1 & \text{for odd-odd nuclei.} \end{cases}$$

This formula is called *semi-empirical* because it is based on both experimental data and theoretical reasoning. The first term is proportional to the mass number, meaning that the larger the "volume" of the droplet, the more bound it is. However, as the volume increases, so does the surface area, leading to greater surface tension, which is why the second term is proportional to the "surface area" of the droplet. The third term accounts for the Coulomb repulsion between protons. The fourth term indicates that nuclei with equal numbers of protons and neutrons are the most bound, which is a consequence of the Pauli exclusion principle. Finally, the fifth term accounts for the pairing effect in nuclei. The coefficients of the Weizsäcker formula are derived from experimental data. Overall, the formula provides a reasonably good fit to the plot in Figure 1.

Using the Weizsäcker formula (1), we can estimate the energy released in a single fission event. Suppose a nucleus with mass number $A = 220$ splits into two equal fragments with $A_2 = 110$. In this case, the binding energy per nucleon of the fragments increases by approximately $\Delta\varepsilon \approx 0.8$ MeV (from $\varepsilon_1 \approx 7.6$ MeV for a nucleus with $A = 220$ to $\varepsilon_2 \approx 8.4$ MeV for a nucleus with $A_2 = 110$). Consequently, the released energy is estimated as

$$E \approx A(\varepsilon_2 - \varepsilon_1) \approx 220(8.4 - 7.6)\ \text{MeV} \approx 180\ \text{MeV}. \tag{2}$$

The energy E released in a single fission event can also be obtained directly from formula (1). For two fragments with mass number $A_2 = A/2$, it is determined by the relation

$$E = 2W(A/2, Z/2) - W(A, Z), \tag{3}$$

where substituting equation (1) for W and W_2, assuming $Z = 90$ and neglecting the last term $a_5 \frac{\delta}{A^{-3/4}}$ (due to its small contribution), we obtain:

$$E = a_2 A^{2/3}(1 - \sqrt[3]{2}) + a_3 \frac{Z^2}{A^{1/3}}\Big(1 - \frac{1}{\sqrt[3]{4}}\Big) \approx a_3 \frac{Z^2}{A^{1/3}} \cdot 0,37 - a_2 A^{2/3} \cdot 0.26 \approx$$
$$\approx 350 - 170 = 180\ \text{MeV}$$

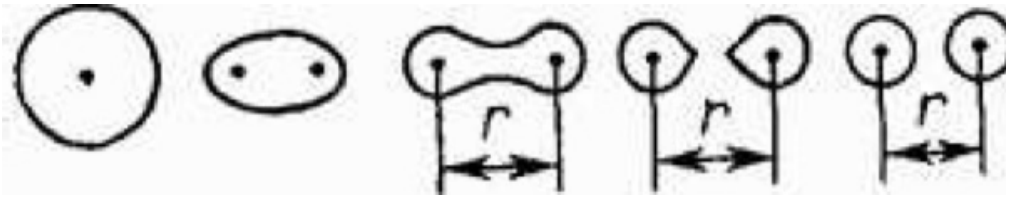

Figure 2. Change in the shape of a nucleus during fission.

Thus, during fission, both the surface energy $E_s = a_2 A^{2/3}$ and the Coulomb energy $E_C = a_3 \frac{Z^2}{A^{1/3}}$ change significantly – the surface energy increases, while the Coloumb energy decreases. Fission is only possible if $E > 0$, i.e., when:

$$\frac{E_C}{E_s} = \frac{a_3}{a_2} \frac{Z^2 A^{1/3}}{A^{2/3}} > 0.7, \tag{4}$$

which means $Z^2/A > 17$. The quantity Z^2/A is called the fission parameter. The energy E released during fission increases with Z^2/A. For $Z^2/A = 17$ this corresponds to ${}^{89}_{39}\mathrm{Y}$ (yttrium).

As seen from these estimates, fission is energetically favorable for all nuclei heavier than yttrium. Why, then, are most nuclei stable against spontaneous fission? To answer this question, we must examine the mechanism of fission.

During fission, the shape of the nucleus changes. The nucleus sequentially passes through the following stages (Fig. 2): Sphere $\rightarrow$ Ellipsoid $\rightarrow$ Dumbbell $\rightarrow$ Two pear-shaped fragments $\rightarrow$ Two spherical fragments. How does the nuclear potential energy change at different stages of fission?

Let us consider the initial stage of fission. As the parameter r increases, the original nucleus takes the shape of an increasingly elongated ellipsoid of revolution. In this case, the change in the nucleus' potential energy due to deformation is determined by the sum of its surface energy and Coulomb energy $E_s + E_C$. It is usually assumed that the volume of the nucleus remains constant during deformation. The surface energy increases because the surface area of the nucleus grows. The Coulomb energy decreases because the average distance between protons increases. Suppose a spherical nucleus undergoes a slight deformation characterized by a small parameter χ, taking the form of an axially symmetric ellipsoid. The surface energy E_s and Coulomb

energy E_C change as functions of χ in the following way (for small χ):

$$\widetilde{E}_s(\chi) \approx \widetilde{E}_s \left(1 + \frac{2}{5}\chi^2\right), \tag{5}$$

$$\widetilde{E}_C(\chi) \approx \widetilde{E}_C \left(1 - \frac{1}{5}\chi^2\right). \tag{6}$$

and their sum, which determines the change in the nucleus' potential energy, is equal to

$$\widetilde{E}_s + \widetilde{E}_C \approx E_s + E_C + \frac{\chi^2}{5}(2E_s - E_C). \tag{7}$$

In relations above E_s and E_C are the surface and Coulomb energies of the original nucleus.

For heavy nuclei, $2E_s > E_C$ and the sum of the surface and Coulomb energies increases with χ. From the previous expressions it follows that, for small deformations, the growth of surface energy opposes further changes in the nucleus' shape and, consequently, fission.

Relation (7) is valid for small values of χ (small deformations). If the deformation is so large that the nucleus takes on a dumbbell shape (region $d_1 < r < d_2$, where $d_{1,2}$ are the maximum size of the deformed nucleus and the sum of the fragment radii, respectively), then the surface and Coulomb forces tend to split the nucleus and give the fragments a spherical shape. At this stage of fission, an increase in deformation leads to a decrease in both Coulomb and surface energies. Thus, as the nuclear deformation gradually increases, its potential energy passes through a maximum. The graph of the change in the nucleus' surface and Coulomb energies as a function of r is shown in Fig. 3.

The presence of a potential barrier prevents the instantaneous spontaneous fission of nuclei. For a nucleus to undergo fission, it must be supplied with energy Q exceeding the barrier height H. The maximum potential energy of a fissioning nucleus is on the order of e^2Z^2/d_2. For example, in the fission of a gold nucleus into two identical fragments, $e^2Z^2/d_2 \approx 173$ MeV, while the energy E released during fission (see formula (3)) is 132 MeV. Thus,

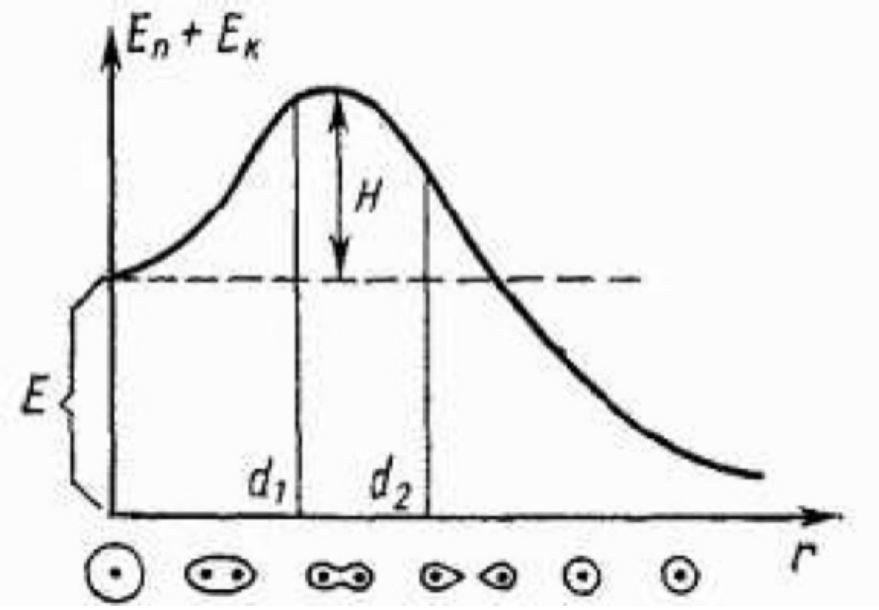

Figure 3. Change in the surface and Coulomb energies of a nucleus during fission.

the fission of a gold nucleus requires overcoming a potential barrier of about 40 MeV.

The fission barrier height H increases as the ratio of Coulomb to surface energy (E_C/E_s) in the initial nucleus decreases. This ratio, in turn, grows with an increase in the fission parameter Z^2/A (see 6). The heavier the nucleus, the lower the fission barrier H, since the fission parameter – assuming Z is proportional to A – increases with the mass number:

$$\frac{E_C}{E_s} = \frac{a_3}{a_2}\frac{Z^2}{A} \sim A. \tag{8}$$

Ultimately, heavier nuclei generally require less energy to be supplied to induce fission.

The fission barrier height vanishes when $2E_s - E_C = 0$. In this case,

$$\frac{2E_s}{E_C} = 2\frac{a_2}{a_3}\frac{A}{Z^2} = 1, \tag{9}$$

from which

$$\frac{Z^2}{A} = \frac{2a_2}{a_3} = \frac{2 \cdot 17.8}{0.7} = 49. \tag{10}$$

Thus, according to the liquid-drop model, nuclei with $Z^2/A > 49$ cannot exist in nature, as they should undergo spontaneous fission almost instantaneously (on the nuclear timescale of about 10^{-22} s). The dependencies of the shape and height of the potential barrier H, as well as the fission energy, on the parameter Z^2/A are shown in Fig. 4.

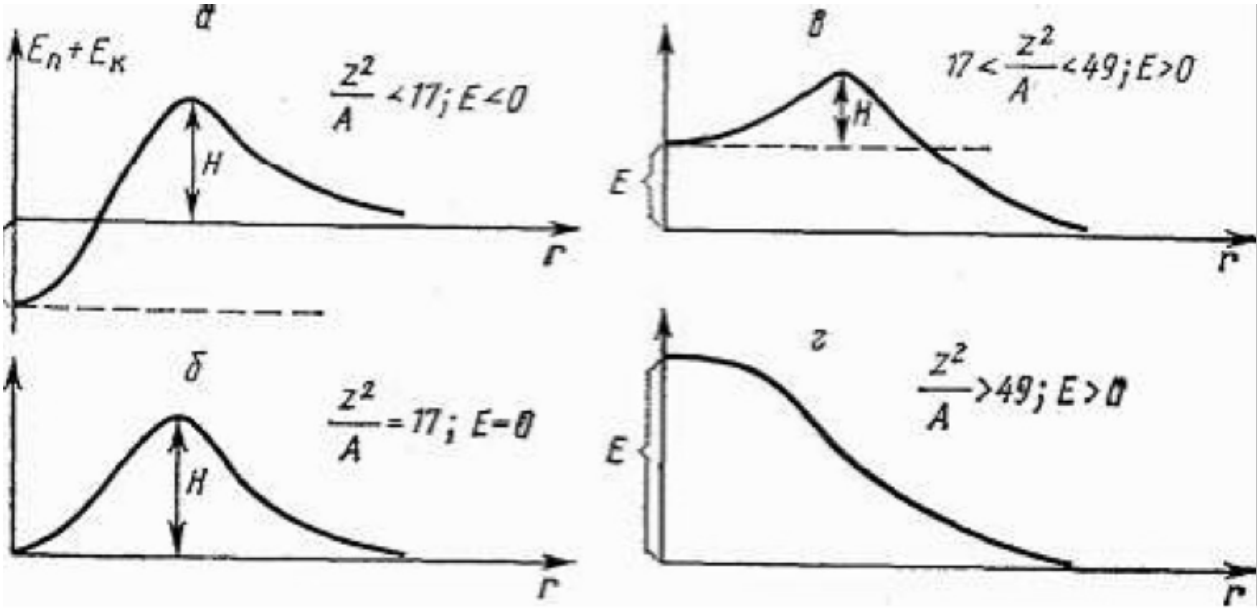

Figure 4. Radial dependence of the shape and height of the potential barrier and the fission energy E for different values of the parameter Z^2/A. The vertical axis represents the quantity $E_s + E_C$.

Spontaneous fission of nuclei with $Z^2/A < 49$, for which the barrier H is nonzero, is impossible from the standpoint of classical physics. However, in quantum mechanics, such fission is possible due to the tunneling effect. The theory of this process was first developed for alpha decay by G.A. Gamow in 1928. In this framework, the nucleus is treated as a system consisting of a core nucleus and an alpha particle. Similarly, one can consider a system of two fission fragments. One of the fragments passes through the potential barrier with a certain probability (see Fig. 5). This process is called spontaneous fission.

The probability of spontaneous fission increases with the fission parameter Z^2/A, i.e., with decreasing fission barrier height. In general, the half-life for spontaneous fission decreases when moving from lighter to heavier nuclei – from $T_{1/2} > 10^{21}$ years for $^{232}_{90}$Th to 0.3 s $^{260}_{104}$Rf.

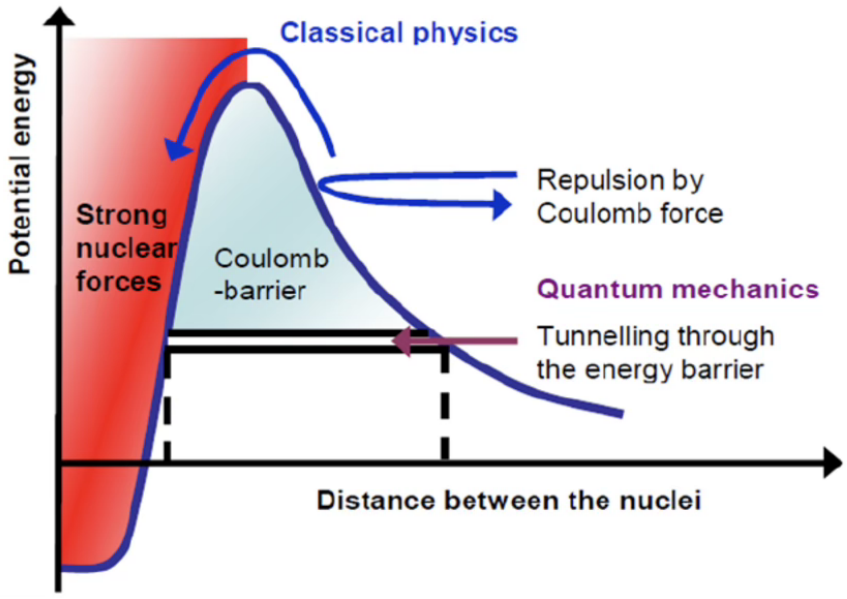

Figure 5. Tunneling through the potential barrier. (Image placeholder)

Induced fission of nuclei with $Z^2/A < 49$ can be triggered by their excitation by any particles – photons, neutrons, protons, deuterons, α-particles, etc. – provided their energy is sufficient to overcome the fission barrier.

4. General Information About Nuclear Fission

A characteristic feature of nuclear fission is that the resulting fragments typically have significantly different masses. In the case of the most probable fission of $^{235}_{92}$U, the mass ratio of the fragments is on average ≈ 1.5. The mass distribution of fission fragments of $^{235}_{92}$U from thermal neutron-induced fission is shown in Fig. 6. For the most probable fission, the heavy fragment has a mass number of 139, while the light fragment has a mass number of 95. Among the fission products, fragments with mass numbers $A = 72 - 161$ and atomic numbers $Z = 30 - 65$ are observed. The probability of fission into two equal-mass fragments is not zero. However, in thermal neutron-induced fission of ^{235}U, the probability of symmetric fission is approximately three orders of magnitude lower than that of the most probable asymmetric fission yielding fragments with $A = 139$ and 95.

The liquid-drop model does not exclude the possibility of asymmetric fis-

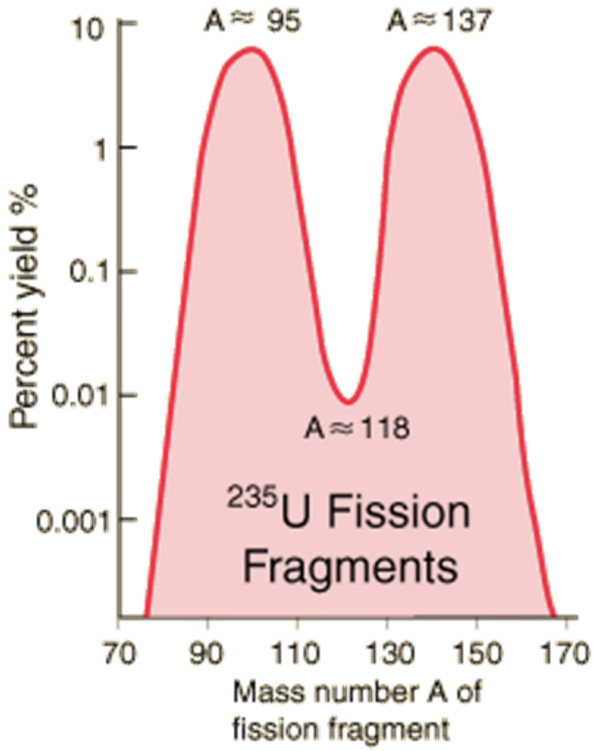

Figure 6. Mass distribution of fission fragments of ^{235}U from thermal neutron-induced fission.

sion, but it does not even qualitatively explain the fundamental patterns of such fission. Asymmetric fission is explained by the shell structure of the nucleus. The nucleus tends to divide in such a way that most nucleons in each fragment form the most stable magic core.

During fission, most of the energy released appears as the kinetic energy of the fission fragments. This conclusion can be drawn from the fact that the Coulomb energy of two touching fragments is approximately equal to the total fission energy. Let us estimate the Coulomb energy of two touching fragments:

$$E_C = \frac{(eZ)^2}{2R}, \tag{11}$$

where R is the radius of the fragments, and eZ is their charge. We will assume that R and Z of the fragments are equal. Let the masses of the fragments be

115 and their charge 45. Then:

$$R = 1.25 \cdot A^{1/3} \cdot 10^{-13} \text{ sm } = 1.25 \cdot 10^{-13} \cdot \sqrt[3]{115} \approx 6.1 \cdot 10^{-13} \text{ sm},$$
$$E_C = \frac{45^2 \cdot (4.8 \cdot 10^{-10})^2}{2 \cdot 6.1 \cdot 10^{-13} \cdot 1.6 \cdot 10^{-6}} \approx 240 \text{ MeV}.$$

The following relationship exists between the kinetic energies of the fragments and their masses, derived from the conservation laws of energy and momentum:

$$\frac{T_l}{T_h} = \frac{M_h}{M_l}, \tag{12}$$

where T_l and M_l refer to the light fragment, and T_h and M_h refer to the heavy one. Using this relation, one can obtain the energy distribution of the fragments from their mass distribution (Fig. 7).

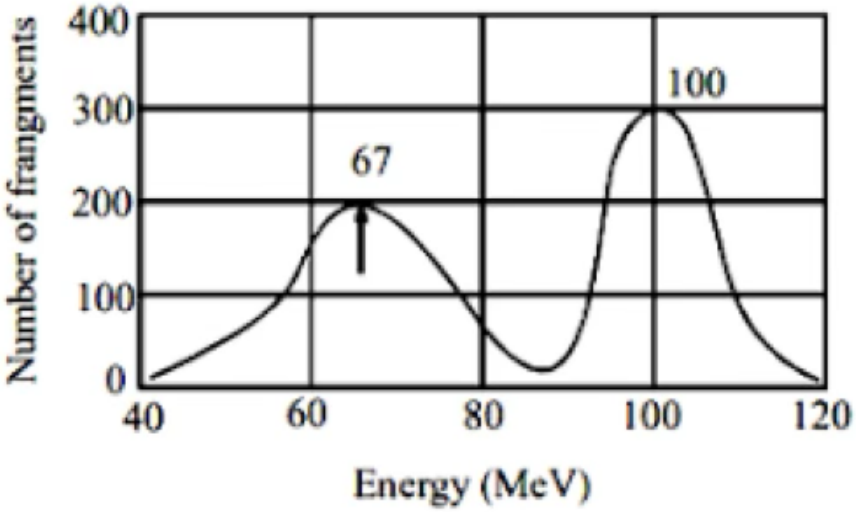

Figure 7. Energy distribution of fission fragments of ^{235}U induced by thermal neutrons.

The parameters of the energy distribution, as well as some other characteristics of the fission fragments of ^{235}U induced by thermal neutrons, are given in Table 1.

It should be noted that the kinetic energy of the fragments obtained through calorimetric measurements does not agree, within error margins, with the values obtained using methods based on measuring ionization in detector material – such as an ionization chamber or semiconductor detector. For in-

Table 1. Characteristics of Light and Heavy Fragments for the Most Probable Thermal Neutron-Induced Fission of ^{235}U.

Characteristic	Light Fragment	Heavy Fragment
Kinetic energy, MeV	100	67
Mass number	95	139
Atomic number	38	54
Initial total charge (in electron charge units)	+20	+22
Range in air at normal conditions, mm	27	21

stance, the kinetic energy of each fragment measured with a semiconductor detector, depending on the detector's quality, may be $5-20$ MeV lower than the tabulated value. This phenomenon is known as the ionization defect, and its essence is as follows.

Fission fragments, having a very high specific ionization energy, generate such a high density of electron-hole pairs along their track in the detector that the fragment's path essentially becomes a plasma region. The weak penetration of the external electric field into this electron-hole plasma leads to insufficiently fast initial track dispersion and significant recombination of the initially generated electron-hole pairs.

During thermal neutron-induced fission of ^{235}U, approximately 200 MeV of energy is released. Of this, 167 MeV is carried away as the kinetic energy of the fragments. The remaining energy (33 MeV) is distributed among various types of radiation arising during the fission process and the radioactive decay of the fragments (Table 2).

Table 2. Distribution of Fission Energy (in MeV) Among Various Products.

Product	Energy (MeV)
Kinetic energy of fission fragments	167
Energy of fission neutrons	5
Energy of β^- particles from fission products	5
Energy of prompt γ-radiation	7
Energy of γ-radiation from fission products	6
Energy of antineutrinos from fission products	10
Total fission energy	200

The neutron-to-proton ratio (N/Z) in nucleus ^{235}U is 1.55, whereas in stable elements with masses close to those of fission fragments, this ratio ranges between 1.25 and 1.45. Consequently, fission fragments are highly neutron-rich and must undergo β^- decay. In fact, fission fragments typically undergo a series of successive β^- decays, with the charge of the primary fragment potentially changing by 4 to 6 units. Below is a typical decay chain of $^{97}_{36}$Kr, one of the fragments produced in the fission of ^{235}U:

$$^{97}_{36}\mathrm{K} \xrightarrow{\beta^-} {}^{97}_{37}\mathrm{Rb} \xrightarrow{\beta^-} {}^{97}_{38}\mathrm{Sr} \xrightarrow{\beta^-} {}^{97}_{39}\mathrm{Y} \xrightarrow{\beta^-} {}^{97}_{40}\mathrm{Zr} \xrightarrow{\beta^-} {}^{97}_{41}\mathrm{Nb} \xrightarrow{\beta^-} {}^{97}_{42}\mathrm{Mo}.$$

De-excitation of fission fragments, caused by the disruption of the normal proton-to-neutron ratio characteristic of stable nuclei, also occurs through the emission of prompt fission neutrons. These neutrons are emitted by the moving fragments in less than $\sim 10^{-14}$ s. On average, 2–3 prompt neutrons are emitted per fission event. Their energy spectrum is continuous, with a peak around 1 MeV. The average energy of a prompt neutron is close to 2 MeV. The emission of more than one neutron per fission event enables energy generation through a self-sustaining nuclear fission chain reaction.

A small fraction ($\sim 1\%$) of the neutrons emitted during fission appear with some delay relative to the moment of fission (so-called delayed neutrons). In some fragments, the delay time can reach up to 1 minute. It has been established that delayed neutrons are emitted by stopped fragments following a preceding β^- decay. The β^- decay of fragments leads to the formation of daughter nuclei not only in the ground state but also in excited states. If the excitation energy exceeds the neutron separation energy $B(n)$, delayed neutron emission occurs (Fig. 8).

Part of the fission energy is carried away by γ quanta emitted by excited fragments immediately after the emission of prompt neutrons (so-called prompt fission γ rays), as well as by γ quanta emitted after the β decay of the fragments.

About 5% of the fission energy is carried away by antineutrinos produced during the β decay of the fragments.

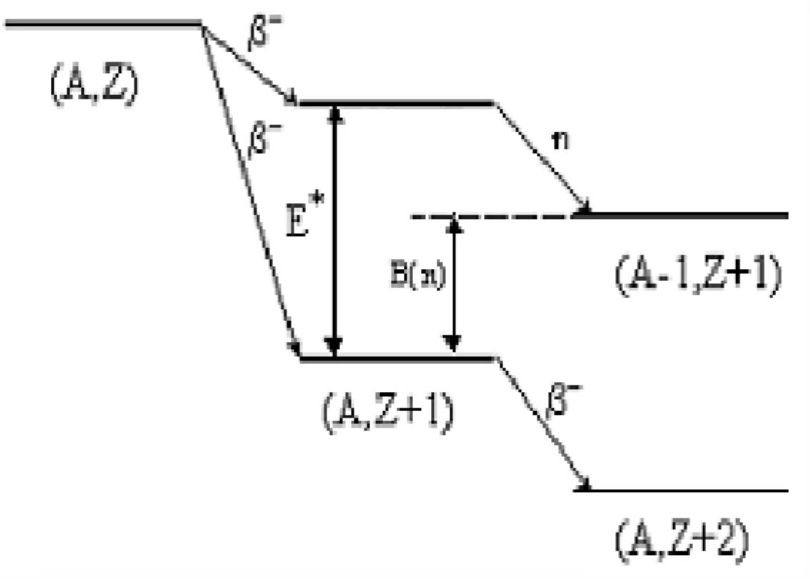

Figure 8. Diagram of delayed neutron formation: E^* – excitation energy of the nucleus $(A, Z+1)$; $B(n)$ – neutron separation energy in the nucleus $(A, Z+1)$; E_n — kinetic energy of the delayed neutron.

Neutrons generated in fission reactions have a kinetic energy of several MeV. For applications such as induced fission of uranium, typically done by means of a chain reaction (where neutrons emitted in one act of fission cause more such reactions), it is necessary to slow the neutrons down to increase the effective cross-section of fission. In this case, the effective reaction cross-section increases as the velocity v of the incident particle decreases, following the law $\sigma \sim 1/v$. To slow down neutrons, elastic scattering of neutrons on atomic nuclei is used. The energy loss of neutrons is maximized in elastic scattering on light nuclei. For example, on protons, a neutron loses, on average, half of its energy in a single scattering event. In elastic scattering on heavier nuclei, the average kinetic energy loss of the neutron is smaller than in scattering on protons. For instance, in neutron scattering on carbon nuclei, about one-fifth of their energy is lost per scattering event on average. The reduction of neutron kinetic energy through scattering processes continues until the neutrons reach energies comparable to the thermal motion energy of molecules in the moderator material. In this energy range, the neutron energy distribution closely resembles the Maxwellian distribution. The average kinetic energy of thermal neutrons at a moderator temperature

of about $T \approx 300$ K is $\overline{E} \approx k_B T \approx 0.025$ eV. Thus, any hydrogen-containing substance – such as water, paraffin, etc. – can be used as a moderator. However, in some applications of neutron physics, such as sustaining a chain fission reaction, it is essential that the moderator has a low (compared to the effective fission cross-section) effective neutron capture cross-section. Based on these characteristics, good moderators include heavy water (D_2O) and graphite.

In this work, however, only spontaneous fission is studied, meaning the decay occurs on its own and neutrons are not required to cause a chain reaction.

5. Semiconductor Detectors

The setup uses a silicon semiconductor detector. Semiconductor detectors are widely employed for detecting and performing spectrometry of charged particles and gamma rays due to their high energy resolution, fast signal rise time, and compact size. These detectors function as solid-state (crystalline) ionization chambers, where ionizing radiation absorption generates charge carriers – electrons and holes. Unlike an ionization chamber, in a semiconductor detector, electrons are excited not into a continuous spectrum but from the valence band to the conduction band.

Silicon and germanium are typically used for semiconductor detectors. Silicon detectors usually operate at room temperature, while germanium detectors require cooling to approximately 80 K. For charged particle detection, silicon detectors and high-purity germanium (HPGe) detectors are used. Germanium detectors are employed for gamma ray detection, whereas silicon detectors are utilized for X-ray detection.

The schematic of a semiconductor detector is shown in Fig. 9.

In a semiconductor detector, a region is created where there are no free charge carriers – the depleted (sensitive) region. A charged particle passing through the depleted region of the detector generates electron-hole pairs along its trajectory. The average energy required to create one electron-hole pair

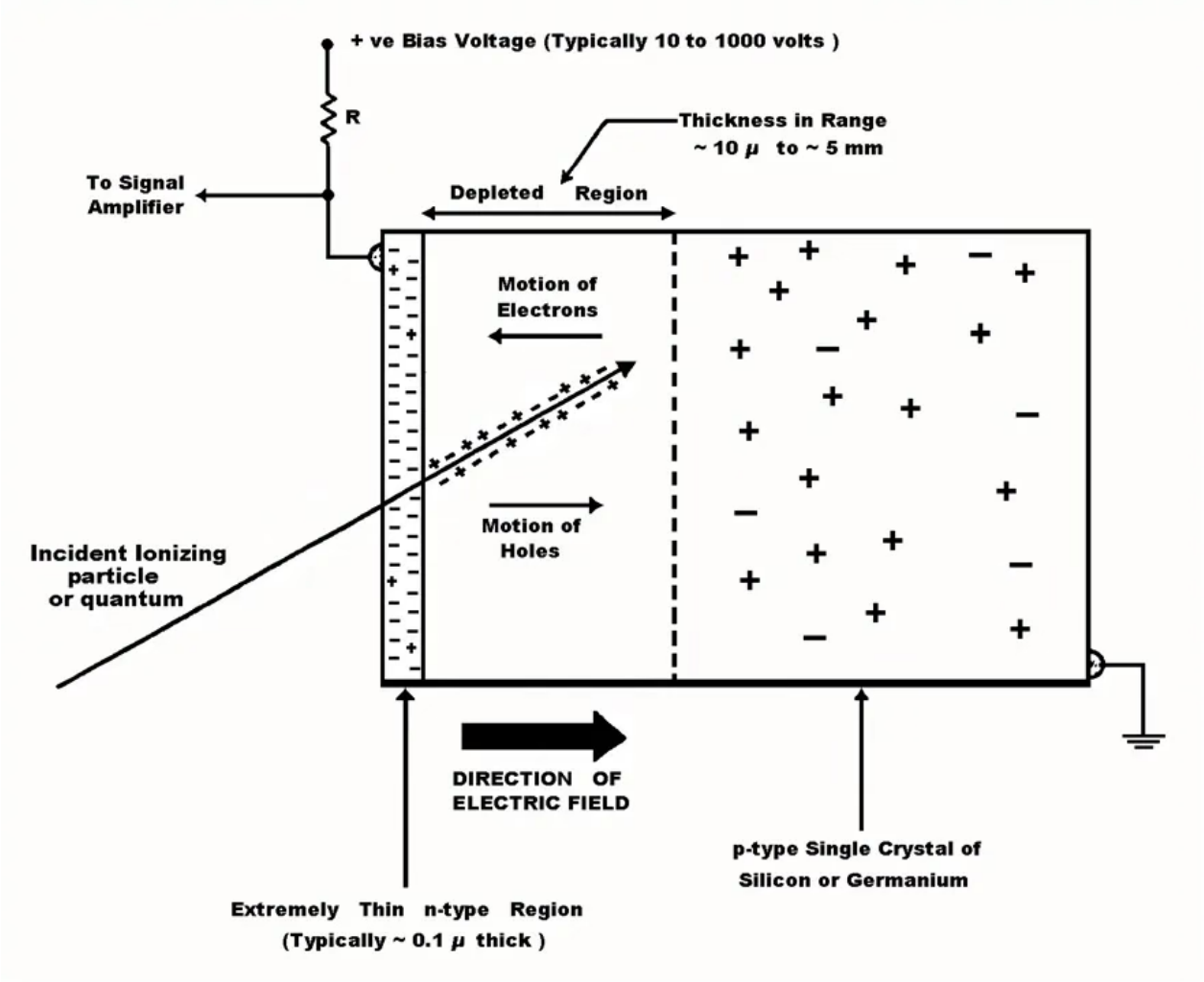

Figure 9. Semiconductor detector schematic.

is 3.62 eV for silicon at room temperature and 2.95 eV for germanium at 80 K. The number of electron-hole pairs is proportional to the energy loss of the particle. To measure the particle's energy, it must lose all its energy and stop within the sensitive region. Under the influence of the electric field applied to the detector, electrons move toward the anode, and holes move toward the cathode. The collected charges form a current pulse, the integral of which carries information about the energy the particle lost in the sensitive region. The detector's current pulse is fed into a charge-sensitive preamplifier and then into an ADC. The ADC generates a number linearly dependent on the amplitude of the amplifier signal. Thus, the number generated by the ADC is proportional to the particle's energy. This number is used to address a memory cell (channel) corresponding to a specific amplitude range.

The channels are sequentially numbered so that higher amplitudes correspond to higher channel numbers. As statistics are accumulated, a distribution (amplitude spectrum) is formed in the computer memory – a dependence of the number of events on the channel number.

The energy resolution of the "semiconductor detector–preamplifier" system is determined by several factors: statistical measurement accuracy, various types of electrical noise in the depletion region of the crystal and in the preamplifier input circuits, charge fluctuations due to incomplete charge collection, and energy loss fluctuations in the detector's entrance window. For example, for a 5 MeV α particle, the energy resolution is $\sim$ 10–12 keV, i.e., approximately 0.2%.

6. Experimental setup

The recording electronic equipment consists of a charge-sensitive preamplifier, an amplifier, and an analog-to-digital converter (ADC). Pulses from the amplifier are fed into the ADC, which serves as the computer interface (Fig. 10).

The *charge-sensitive preamplifier* is designed to convert information about the charge generated in the detector's sensitive region into a pulse amplitude proportional to the charge.

The *amplifier* amplifies and shapes the signals from the preamplifier.

The *analog-to-digital converter* (ADC) measures pulse amplitudes, i.e., it converts analog information into digital form (generating a number linearly dependent on the input signal amplitude).

An event processed by the ADC is recorded in a specific memory cell (channel) of the computer, corresponding to a certain amplitude range. The channels are numbered sequentially so that higher amplitudes correspond to higher channel numbers. As statistics are accumulated, an energy spectrum ("number of events vs. channel number") is formed in the computer's memory, which can be displayed on a monitor or printed after the measurements are completed.

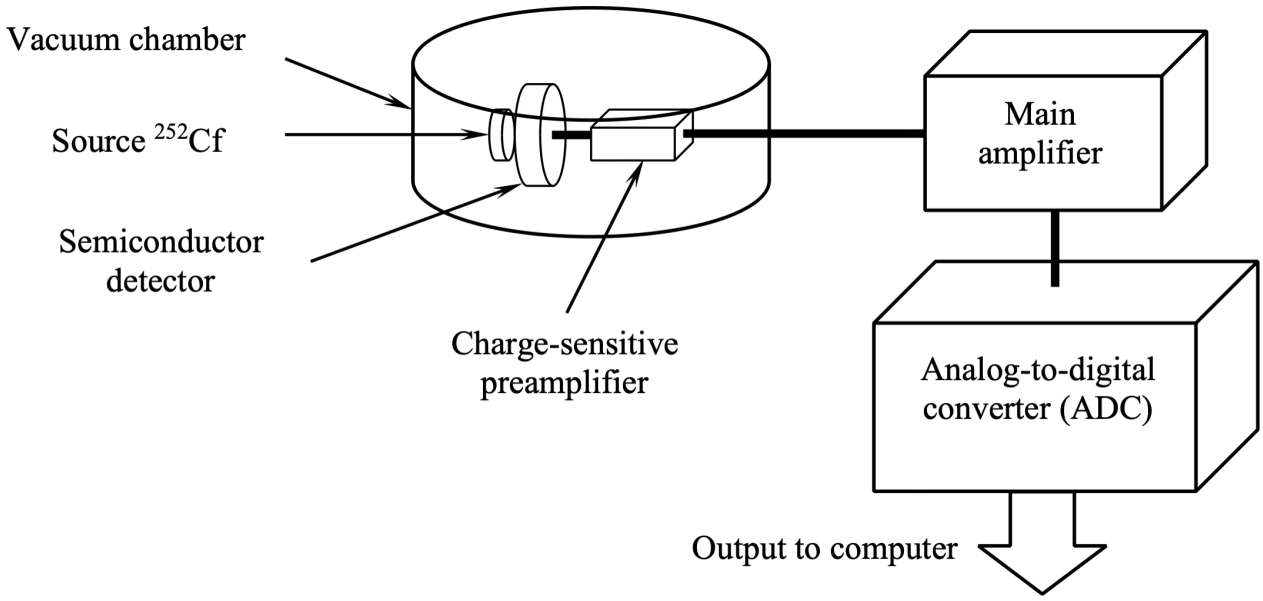

Figure 10. Block diagram of the setup for measuring fission fragment spectra.

The *detector bias* voltage source is necessary to create an electric field under which the charges generated in the detector due to ionization produced by the detected particle in the sensitive layer are collected.

The ^{252}Cf source and the detector are placed in a vacuum chamber to prevent the loss of kinetic energy of the fragments due to air ionization. The semiconductor detector is positioned almost in direct contact with the surface of the ^{252}Cf source. The detector surface is parallel to the californium layer surface. The resulting fission fragments are detected by the semiconductor detector. In each fission event, only one of the two fragments is detected, as they fly apart in opposite directions.

7. Experimental procedure

Exercise №1. Measurement of the energy of ^{252}Cf spontaneous fission fragments. Calibration of the spectrometer using symmetric fission energy and associated α decay energy.

The fission fragment spectrum should cover at least 800 channels. The measurement of the fission fragment spectrum should be carried out over a period sufficient to achieve a statistical accuracy of 10% in the peaks of this

spectrum (see Fig. 11). This may take more than an hour. After completing the measurement, the obtained results must be saved and printed, and the duration of the measurement should also be recorded.

Figures 11 and 12 show two spectra of ^{252}Cf spontaneous fission fragments, corresponding to two different acquisition times. The spectrum in Fig. 11 corresponds to an acquisition time of $\sim$ 2 hours, while the one in Fig. 12 corresponds to $\sim$ 6 hours. It can be observed that with increasing measurement time, the relative statistical error in the spectrum decreases, the mass distribution of the fission fragments becomes more distinct, and the accuracy of determining the positions of the peaks and valleys in the fission fragment spectrum improves.

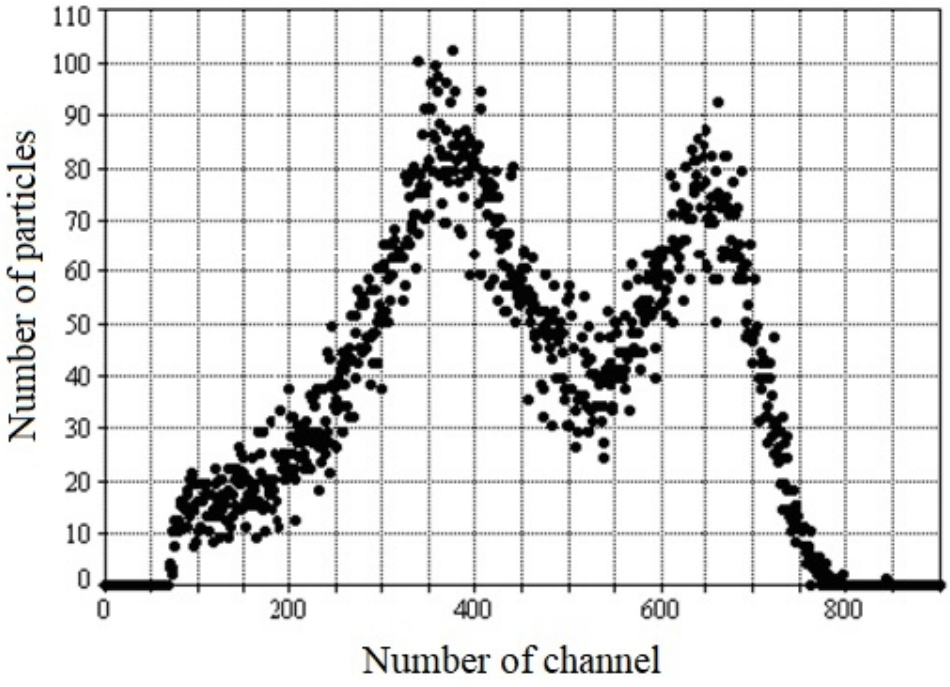

Figure 11. Spectra of fragments from the spontaneous fission of ^{252}Cf. Acquisition time: 2 hours.

The spectrometer is calibrated in two ways: using the energy of the symmetric fission of ^{252}Cf and using the α decay line.

The symmetric fission into two identical fragments corresponds to the central minimum of the energy spectrum. The total kinetic energy of the ^{252}Cf fission fragments is 181 MeV. For calibration, it is necessary to determine the

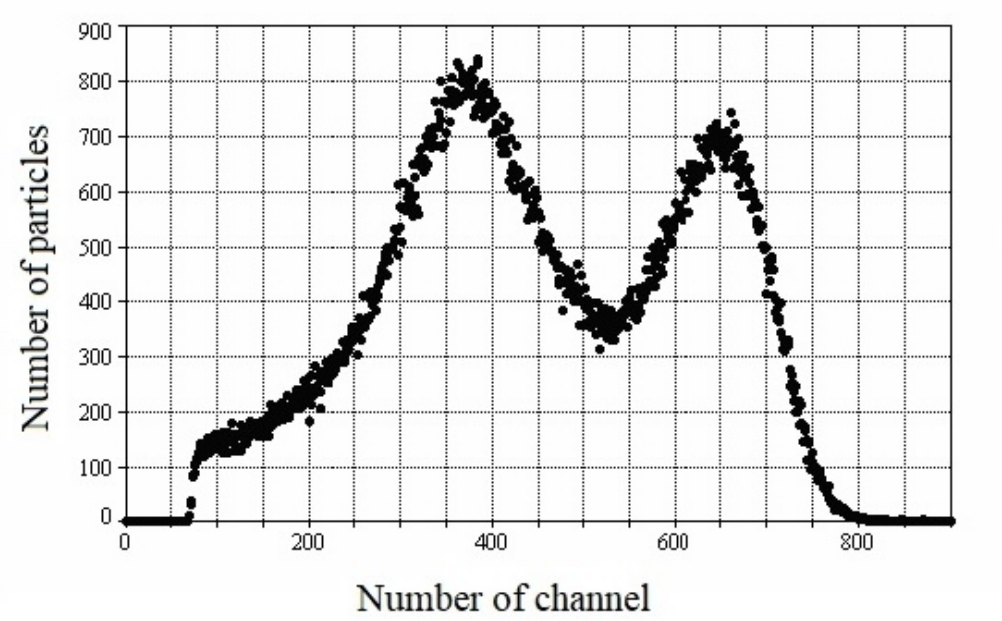

Figure 12. Spectra of fragments from the spontaneous fission of ^{252}Cf. Acquisition time: 6 hours (example).

position of the minimum in the obtained fragment spectrum.

An alternative calibration method is based on the kinetic energy of the α particles released in α decay of ^{252}Cf. The kinetic energy of the α particles emitted by ^{252}Cf is 6.12 MeV.

Exercise №2. Determining the ratio of the decay probabilities of ^{252}Cf via the alpha decay and spontaneous fission channels.

This exercise uses the measurement results from the first exercise.

The measurement results must be presented in the form of graphs of the energy spectra of alpha particles and fission fragments of ^{252}Cf. It is necessary to determine the values of the absolute (ΔE_α) and relative ($\Delta E_\alpha / E_\alpha$) energy resolution of the setup. The absolute energy resolution ΔE_α is defined as the full width at half maximum (FWHM) of the alpha particle peak. Based on the data from the first exercise, the amplitude analyzer's channel scale is calibrated, i.e., the dependence of energy on the channel number of the amplitude analyzer is determined. It is assumed that channel zero corresponds to zero energy in the spectrum. The second point for the calibration curve is determined in one case from the position of the symmetric fission minimum

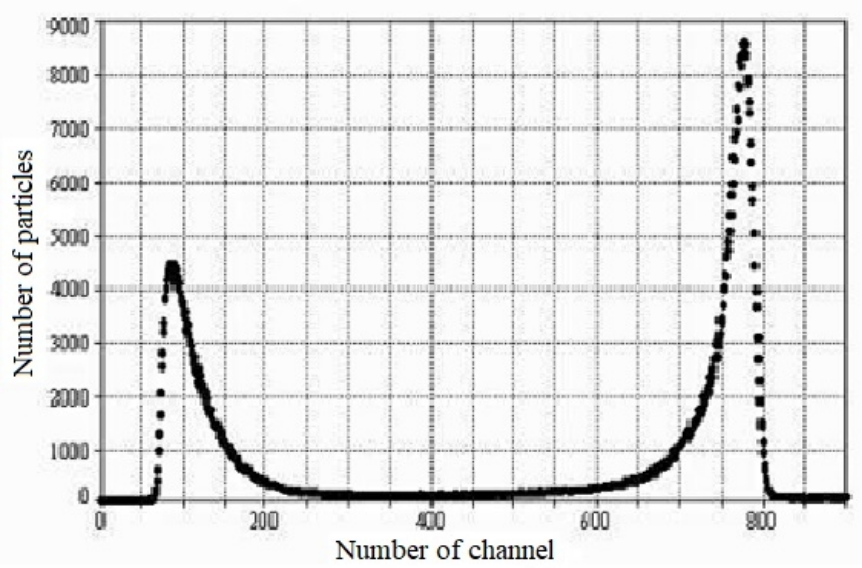

Figure 13. Alpha spectrum of ^{252}Cf. Acquisition time: 13 minutes (example).

in the fission fragment spectrum (total kinetic energy of the fragments is 181 MeV), and in the other case from the position of the maximum in the ^{252}Cf alpha spectrum with an energy of 6.12 MeV.

Based on the measured energy spectrum of fission fragments, the most probable kinetic energies of the light and heavy fragments are determined. To obtain the correct energy values from the measured ones, several corrections must be applied:

- A correction for energy loss as fission fragments pass through the detector's coating (gold or another material).
- A correction for the ionization defect – recombination of positive ions and electrons due to the high ionization density along the fragment's track. The magnitude of the recombination correction is approximately the same for light and heavy fragments and amounts to 3–5 MeV.

The specific values and calculation methodology for these corrections are provided in the laboratory setup instructions. These corrections are added to the kinetic energy of each fragment obtained from the experiment, after which their masses are determined using formula (12). For the total mass of

the fragments, the relation $M_l + M_h = 252 - 2$ should be used, where 2 is the most probable number of prompt fission neutrons.

It is necessary to estimate the accuracy with which the most probable kinetic energies of the light and heavy fragments are determined from the experimentally measured fission fragment energy spectrum. This accuracy depends on two factors:

- The accuracy of the analyzer scale calibration.
- The uncertainty in the position of the maxima of the fission fragment energy spectrum, due to the statistical accuracy of the measurements and the accuracy of the corrections.

It should be remembered that the uncertainty in the position of the fragment spectrum maxima cannot be found as the full width at half maximum of each of these maxima, since the shape of the fragment spectrum reflects the real distribution of kinetic energies of the fission fragments produced.

The ratio of the decay probabilities via different channels and the determination of the spontaneous fission branch ratio in the decay of ^{252}Cf should be calculated from the integrals of the obtained spectra. Given the linearity of the spectrometer channel, the integral is proportional to the sum of all counts in the respective spectrum. The measurement time for each spectrum must be taken into account, as the decay probability is inversely proportional to its intensity.

To submit the work, provide:

- Graphs of the energy spectra of fission fragments and alpha particles.
- Calculated positions of the maxima in the fission fragment energy spectra with an estimate of the experimental measurement error.
- Calculated most probable masses of the light and heavy fragments with an estimate of the measurement errors.

- Calculated values for the energy loss corrections due to the ionization defect and the passage of fragments through the detector's protective layer.
- Calculated absolute and relative energy resolution of the ^{252}Cf alpha spectrum.
- Calculated ratio of the decay probabilities via the spontaneous fission and alpha decay channels, and the spontaneous fission branch ratio in the decay of ^{252}Cf.